第 29 卷 第 9 期 焊 接 学 报 Vol. 29 No. 9
2008 年 9 月 TRANSACTIONS OF THE CHINA WELDING INSTITUTION September 2008

弧焊机器人结构光视觉传感焊缝跟踪

张广军， 冷孝宇， 吴 林
（哈尔滨工业大学 现代焊接生产技术国家重点实验室，哈尔滨 150001）

摘 要：建立了弧焊机器人视觉传感焊缝跟踪系统，重点研究了跟踪路径提取算法和焊缝跟踪的实现策略。采用传感器引导机器人运动的控制方式，为克服前视距离的影响，提取的焊缝跟踪点信息在跟踪过程中不是立刻被使用的，而是存储在循环队列结构中，要等到焊枪到达该点附近时才能用到。计算出的机器人驱动向量使焊枪向焊缝的中心点方向调整，并按照给定的步长运动，使其始终沿焊缝方向向前运动，实现沿焊缝的自主跟踪。结果表明，通过对焊枪位置及绕焊枪旋转角度的调节，实现了 S 形曲线焊缝的实际跟踪，跟踪过程平稳、精确。

关键词：焊缝跟踪；视觉传感；结构光；弧焊机器人
中图分类号：TG115.28 文献标识码：A 文章编号：0253—360X(2008)09—0008—03

张广军

0 序 言

目前国内外应用的弧焊机器人主要采用示教再现方式，示教再现式比较简单、直观、易于操作。但是，在实际应用中焊件受热引起形变，或由于大型焊件焊缝开口一致性不好，采用再现就难以保证焊接质量[1]。为适应环境的变化，需要研究带有传感器的智能化机器人焊接。因此对焊缝跟踪方法和技术的研究已成为机器人在焊接应用研究中的一个热点[2]。

与其它传感器相比，结构光视觉传感器具有提供信息量丰富，灵敏度和测量精度高，抗电磁场干扰能力强，与工件无接触的优点，适合于各种坡口形状，是最有前途的一种焊缝跟踪传感器[3-6]。

从实用的角度出发，采用结构小巧、紧凑的结构光视觉传感器，安装在自行研制的 HRGH—4 弧焊机器人上，并实现了焊缝的自主跟踪。

1 焊缝跟踪试验系统

所研制的弧焊机器人结构光视觉传感焊缝跟踪系统如图 1 所示，主要由以下几个部分组成。

（1）结构光传感系统：包括 CCD 摄像机、激光器、DH—CG210 图像采集卡、激光器电源、摄像机电源等。

（2）HRGH—4 弧焊机器人：自行研制的全开放的弧焊机器人。

（3）传感器控制器。

（4）机器人控制系统。

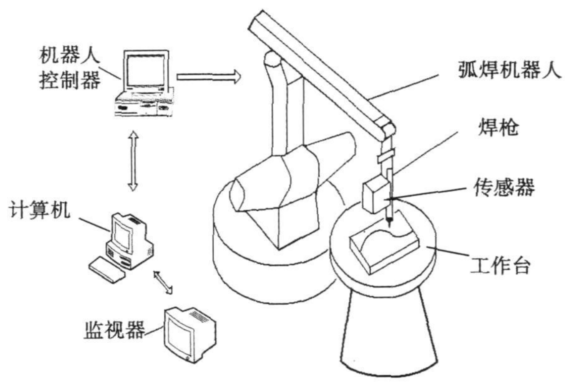

图 1 焊缝跟踪系统

Fig. 1 Robotic welding seam tracing system

结构光跟踪传感器被固定在机器人的焊枪上。传感器采集到坡口上的光纹图像，将模拟视频信号送入图像采集卡，图像卡将视频信号转换成数字图像送入控制计算机，经过图像处理程序提取坡口的特征点坐标，用标定得到的换算关系把特征点图像坐标转化为焊枪工具坐标系下的坐标，然后将得到的坐标值数据传送到机器人控制器，计算出特征点的世界坐标。

这里采用传感器传感引导机器人运动的方式。

收稿日期：2007—10—11
基金项目：国家自然科学基金资助项目(50675046，50775053)

因为传感器投射的结构光纹在焊枪之前有一定距离(称为前视距离),所以提取的特征点信息在跟踪过程中不是立刻被使用的,而要等到焊枪到达该点附近时才能用到。因此需要把采集到的跟踪点信息存储起来,在需要的时候提供使用,文中采用循环队列结构存储跟踪点数据。这样实时由机器人控制器中读取 T6 矩阵,计算被跟踪点在机器人基坐标系下的坐标,将坐标值存入预先建立的循环队列。选择合适的控制算法,由机器人控制器向机器人发出指令,控制机器人沿着焊缝的轨迹行走,实现焊缝跟踪。

2　跟踪路径提取

设前视距离为 $\Delta L = 30$ mm,图像处理时间为 $\Delta T = 90$ ms,所用机器人伺服周期为 $\Delta t = 15$ ms。如果焊接速度为 $V = 5$ mm/s,那么测量点时间间隔为 6 个伺服周期,即0.45 mm。在前视距离长度内,可以采集66 个焊缝特征点。

采用直线拟合来处理局部数据,以消除干扰。图2 示出了每个测量点理想的焊枪位姿的计算方法。图中焊缝上点 c 的坐标是由图像处理和坐标变化得到的。理想的焊枪指向,即 Z_s 方向,应垂直于焊件表面,是表面的法线方向。多个测量点拟合的直线L_1L_2 代表着焊接方向,光纹 ae 位于焊件表面平面内,其方向也是已知的。由 L_1L_2 和 ae 就可计算出Z_s 方向。这样,测量点 c 的位姿就都得到了。

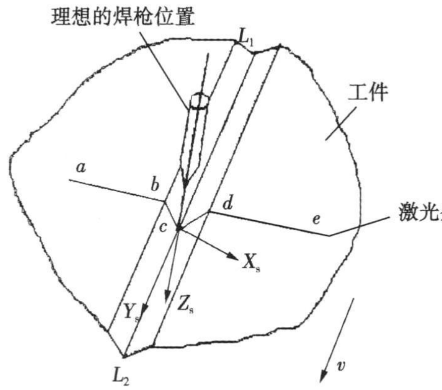

图 2　测量点理想焊枪位姿计算示意图

Fig. 2　Calculation of ideal torch position

3　跟踪的实现

设当前及下一个机器人伺服周期焊枪应到达的位姿矩阵分别表示为

$$\boldsymbol{T}_t(i+1) = \boldsymbol{T}_t(i) \times \Delta \mathrm{T} \tag{1}$$

$$\Delta \boldsymbol{T} = T_t^{-1}(i) \times \boldsymbol{T}_t(i+1) \tag{2}$$

矩阵 $\boldsymbol{T}_t(i+1)$ 是由矩阵 $\boldsymbol{T}_t(i)$ 通过旋转平移而得到的,$\Delta\boldsymbol{T}$ 表示为

$$\Delta \boldsymbol{T} = \mathrm{Trans}(\Delta x, \Delta y, \Delta z) \times \mathrm{Rot}(x, \delta x) \times \mathrm{Rot}(y, \delta y) \times \mathrm{Rot}(z, \delta z)$$
$$= \begin{bmatrix} \cos\delta y\cos\delta z & \cos\delta z\sin\delta y\sin\delta x - \sin\delta z\cos\delta x & \cos\delta z\sin\delta y\cos\delta x + \sin\delta z\sin\delta x & \Delta x \\ \cos\delta y\sin\delta z & \sin\delta z\sin\delta y\sin\delta x + \cos\delta z\cos\delta x & \cos\delta z\sin\delta y\cos\delta x + \sin\delta z\sin\delta x & \Delta y \\ -\sin\delta y & \cos\delta y\sin\delta x & \cos\delta x\cos\delta y & \Delta z \\ 0 & 0 & 0 & 1 \end{bmatrix} \tag{3}$$

由于 δi 很小,存在 $\sin(\delta i) \approx \delta i$, $\cos(\delta i) \approx 1$。式(3)变为

$$\Delta \boldsymbol{T} = \begin{bmatrix} 1 & -\delta z & \delta y & \Delta x \\ \delta z & 1 & -\delta x & \Delta y \\ -\delta y & \delta x & 1 & \Delta z \\ 0 & 0 & 0 & 1 \end{bmatrix} \tag{4}$$

对比式(2) 和式(4) 就可以得到驱动矢量 $\boldsymbol{D}_t$, $\boldsymbol{D}_t = [\Delta x, \Delta y, \Delta z, \delta x, \delta y, \delta z]^T$。机器人的驱动矢量使焊枪向焊缝的中心点方向调整,并按照给定的步长运动,使其始终沿焊缝方向向前运动,实现沿焊缝的自主跟踪。

为保证焊接过程的平稳性,沿着焊接方向每次的调整是固定的,即

$$\Delta y = V \cdot \Delta t \tag{5}$$

驱动矢量的六个分量每次并不是都要调整,这要根据具体情况而定。如跟踪直线焊缝,则只需要调整水平偏差 Δx 和高度偏差 Δy;对于大曲率的曲线焊缝,则有时需要增加焊枪的自转调整,即绕 z 轴旋转,这是由于传感器与焊枪之间有一定的前视距离,而且传感器的视野有限。因此在跟踪过程中,若焊缝轨迹曲率过大,焊缝就会超出传感器的视野范围。因此必须控制焊枪带动传感器绕 z 轴旋转,以控制焊缝始终处在传感器视野范围之内。另外,应尽量控制焊缝的特征点处在结构光纹正中,因为这时在跟踪中产生的误差最小。

4　跟踪试验

对厚度为1.5 mm的S 形薄板对接焊缝进行了焊接跟踪试验,焊接方法为 TIG 焊。

跟踪过程如图 3 所示。

首先使机器人沿焊缝的大致方向匀速前进,当激光条纹打到焊缝时,开始检测出焊缝特征点,图像处理计算机开始向工控机传送数据,陆续将检测到

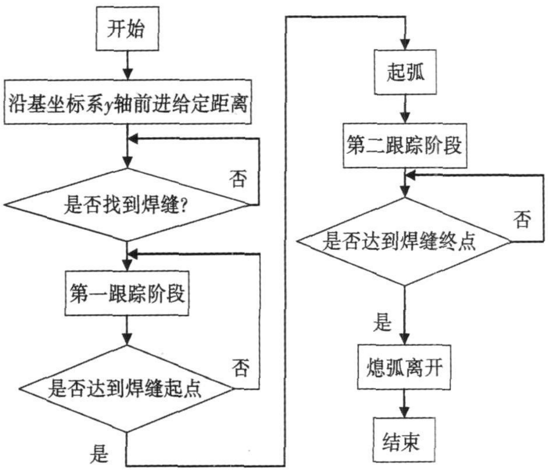

图 3　焊缝跟踪过程示意

Fig. 3　Schematic of seam tracing process

的被跟踪点存入循环队列。在焊枪到达焊缝初始点前的阶段为第一跟踪阶段, 在这个阶段中实时调整焊枪姿态使焊缝始终在激光条纹的中心, 并调整焊枪位置使枪尖与跟踪初始点对中。当焊枪到达初始点时, 焊接开始, 随后进入第二跟踪阶段, 即在焊接状态下控制焊枪沿着焊缝轨迹行走。同时传感器继续采集数据, 发送给机器人控制器并存入循环队列。当焊枪到达焊缝末端时熄弧, 跟踪过程结束。

图 4 是焊接过程中机器人控制器记录的焊枪行走路径。图 5 示出了 S 形焊缝机器人自主跟踪焊接的结果。

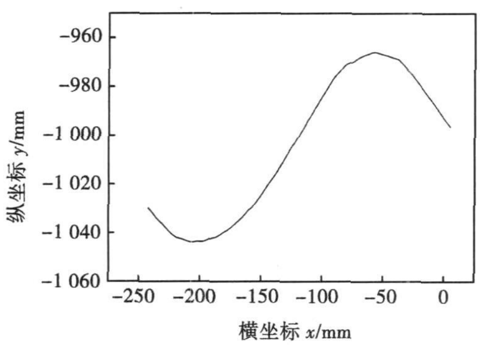

图 4　机器人焊枪运动轨迹

Fig. 4　Path of robot torch

可以看出, 在跟踪曲线焊缝时, 在曲率较大处跟踪平稳, 跟踪曲线平滑。表明该机器人结构光视觉传感系统已初步具备了焊缝跟踪能力。

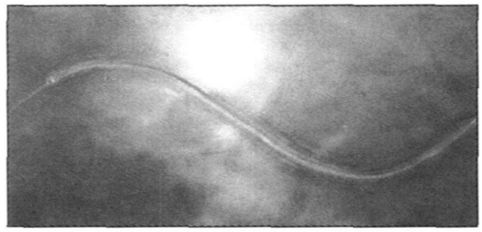

图 5　机器人自主跟踪焊接的 S 形焊件

Fig. 5　S-typed weldpiece by robot seam tracing

5　结　论

所建立的弧焊机器人结构光视觉焊缝跟踪系统实现了焊缝初始点的定位, 自动引导焊枪到达初点, 焊接过程中自主跟踪功能。验证试验结果表明通过对焊枪位置及绕焊枪旋转角度的调节, 实现了 S 形曲线焊缝的实际跟踪, 跟踪过程平稳、精确。

参考文献:

[1]　吴　林, 陈善本. 智能化焊接技术[M]. 北京: 国防工业出版社, 2000.

[2]　王　伟, 邹奇仕, 朱六妹, 等. 视觉传感焊缝跟踪技术的发展状况及实施方案探讨[J]. 电焊机. 2002, 32(5): 1—8.

[3]　张　炯, 吕伟新, 吴　林, 等. 一种弧焊机器人实时激光扫描视觉系统[J]. 高技术通讯, 1996, (5): 40—43.

[4]　孙立新, 戴士杰, 李　慨, 等. 基于线结构光的多道焊跟踪系统图像处理[J]. 焊接学报, 2002, 23(3): 53—55.

[5]　Xu Peiquan, Tang Xinhua, Yao Shun, *et al*. Three-dimension recovery of weld seam for welding robot location based on circular laser vision sensor [J]. Science and Technology of Welding and Joining, 2006, 11(3): 352—357.

[6]　Yul Kang Bae, Jin Hyun Park. A study on development of inductive sensor for automatic weld seam tracking[J]. Journal of Materials Processing Technology, 2006, 176(1—3): 111—116.

作者简介: 张广军, 男, 1969 年出生, 博士, 博士生导师。主要从事机器人与智能化焊接方面的研究。发表论文 80 余篇。

Email: zhanggj@hit.edu.cn

MAIN TOPICS, ABSTRACTS & KEY WORDS

Ultrasonic inspection to detect cold welding in electro-fusion joint of polyethylene pipes

ZHENG Jinyang[1], GUO Weican[1,2], SHI Jianfeng[1], DING Shoubao[2], WANG Hui[1], DING Liangyu[3] (1. Institute of Chemical Machinery and Process Equipment, Zhejiang University, Hangzhou 310027, China; 2. Zhejiang Special Equipment Inspection and Research Institute, Hangzhou 310020, China; 3. Zhejiang Zhongcai Pipes Technical Co. Ltd., Xincang 312500, Zhejiang, China). p1—4

Abstract: Polyethylene (PE) pipe is widely used in the gas distribution networks. Cold welding caused by insufficient input of heat energy, which can not be detected by nondestructive test methods available, is one of the most dangerous defects in the joint of PE pipes. It was discovered that there is an Eigen-line in the electro-fusion (EF) joint of PE pipes due to a great amount of separated micro-bubbles, and the distance between the line and heating wires can be used to measure the degree of cold welding. Furthermore, a unique method was developed to detect cold welding. The degree of cold welding can be assessed with an empirical formula by measuring the distance between the line and metal wires with a proprietary system of ultrasonic inspection. Experiments show that the method can accurately detect cold welding and be used in the research of welding procedure, and quality inspection.

Key words: polyethylene pipe; electrofusion joint; cold welding; ultrasonic testing

Fatigue crack growth rate of A7075 FSW

WANG Xijing, LI Shuwei, NIU Yong, Zhang Jie (State Key Laboratory of Gansu Advanced Non-ferrous Metal Materials, Lanzhou University of Technology, Lanzhou 730050, China). p5—7

Abstract: The fatigue crack growth rate of A7075-T651 aluminum baseplate, FSW welding and heat-affected zone were studied. And A7075-T651 aluminum baseplate were welded with FSW-3LM-015 friction stir welding machine. Fatigue crack growth tests using CT specimen and 810 Material test system for testing machine. Polynomial method obtained by increasing fatigue crack growth rate (da/dN) and (ΔK) respectively, include the base metal and welding zone and the heat-affected zone in the same sample group (da/dN) and (ΔK) combined data points overall regression analysis. Experimental results indicated fatigue crack growth rate of the heat-affected zone is higher than that of the base metal and weld the nuclear area.

Key words: friction stir welding; fatigue crack growth rate; HAZ; A7075-T651 aluminum alloy

Robotic welding seam tracing system based on structure light vision sensor

ZHANG Guangjun, LENG Xiaoyu, WU Lin (State Key Laboratory of Advanced Welding Production Technology, Harbin Institute of Technology, Harbin 150001, China). p8—10

Abstract: A structured-light visual sensing system for seam tracing was built on the arc welding robot, the extract arithmetic of trace path and the realization strategy for seam tracing were mainly researched. The control mode was adopted that sensor guided robot movement. In order to overcome the effect by look-ahead distance, the extracted tracing points were not used immediately, but stored in the circle queue, and they would be used when welding torch was nearby. The calculated driving vector made the welding torch move to the centre point of the welding seam. The torch would move forward at the given step length along the seam all the time, so the autonomous trace was implemented. The validating experiment on tracing S-curve seams by adjusting position and angle of torch proved that the developed system is robust, and the tracing process is stable and accurate.

Key words: seam tracing; visual sensing; structured-light; arc welding robot

TiC_p reinforced titanium composite layer on Ti6Al4v alloy

ZHANG Song[1], GUAN Xiangnan[1], ZHANG Chunhua[1,2], WU Weitao[3], WANG Maocai[3] (1. College of Materials Science and Engineering, Shenyang University of Technology, Shenyang 110178, China; 2. College of Materials and Metallurgy, Northeastern University, Shenyang 110004, China; 3. State Key Laboratory for Corrosion and Protection of Metals, Institute of Metals, Chinese Academy of Sciences, Shenyang 110016, China). p11—14

Abstract: Metal-ceramic composites show many advantages for various industrial applications. It is well known that Ti-based composite possesses quite attractive aspects in physical and chemical properties. In this paper 10wt% of mixed powders of W_2C or Cr_3C_2 and Ti are used respectively, and an in-situ forming TiC/Ti metallic composite layer on Ti6Al4V is fabricated by laser induced reaction. The results show that the microstructure of the composite layer is strongly related with the composition of original powders and also the laser processing parameters. Under certain processing parameters, the TiC particles are fine and uniformly disperse in the composite layer. As different pro-placed metal-ceramic powders, composite bases are made of single-plase α-Ti or single-phase β-Ti respectively.

Key words: in-situ synthesis; TiC particle; titanium matrix metal composite

Traveling control for flying-type flash-butt welder and its simulating analysis

SUN Xinxue[1], FU Yongling[1], LU Ning[1], SUN Mingwu[2] (1. School of Automation Science and Electrical Engineering, Beijing University of Aeronautics and Astronautics, Beijing 100083, China; 2. Capital Construction Office, Hebei Tourism Vocational College, Chengde 067000, Hebei, China). p15—18

Abstract: In order to optimize the control for flying-type flash-butt welder in an EBROS (endless-bar rolling system) before its physical prototype was made, a virtual prototype for the welder had been established. According to welder's working characteristics in the system, a control plan had been used that welder's moving velocity and its displacement were controlled in subsection. In order